Ab initio calculations of light-ion reactions

Petr Navrátil[1,2]*, Sofia Quaglioni*[2]*, Simone Baroni*[3]*, and Robert Roth*[4]
[1]TRIUMF, 4004 Wesbrook Mall, Vancouver, BC V6T 2A3, Canada
[2]Lawrence Livermore National Laboratory, P.O. Box 808, L-414, Livermore, CA 94551, USA
[3]Physique Nucléaire Théorique, Université Libre de Bruxelles, C.P. 229, B-1050 Bruxelles, Belgium
[4]Institut für Kernphysik, Technische Universität Darmstadt, 64289 Darmstadt, Germany

Abstract
In recent years, significant progress has been made in *ab initio* nuclear structure and reaction calculations based on input from QCD employing Hamiltonians constructed within chiral effective field theory. In this contribution, we present one of such promising techniques capable of describing simultaneously both bound and scattering states in light nuclei. By combining the resonating-group method (RGM) with the *ab initio* no-core shell model (NCSM), we complement a microscopic cluster approach with the use of realistic interactions and a microscopic and consistent description of the clusters. We discuss applications to light nuclei scattering, radiative capture and fusion reactions.

1 Introduction

Nuclei are quantum many-body systems with both bound and unbound states. One of the major challenges for theoretical nuclear physics is to provide a unified description of structural and reaction properties of nuclei that is based on the fundamental underlying physics: the constituent nucleons and the QCD-based realistic interactions among them. A predictive theory of reactions of light nuclei is needed for many reasons.

First, it would greatly help our understanding of nuclear reactions important for astrophysics. Some of the outstanding light-nucleus uncertainty sources in astrophysics applications include: reactions leading to the nucleosynthesis of ^{8}B (and the production of the solar neutrinos measured in terrestrial experiments) such as the ^{7}Be$(p,\gamma)^8$B and ^{3}He$(\alpha,\gamma)^7$Be radiative capture rates; the thermonuclear reaction rates of α capture on ^{8}Be and ^{12}C nuclei during the stellar helium burning.

Furthermore, nuclear reactions are one of the best tools for studying exotic nuclei, which have become the focus of the next generation experiments with rare-isotope beams. These are nuclei for which most low-lying states are unbound, so that a rigorous analysis requires scattering boundary conditions. In addition, much of the information we have on the structure of these short-lived systems is inferred from reactions with other nuclei.

Finally, low-energy fusion reactions represent the primary energy-generation mechanism in stars, and could potentially be used for future energy generation on earth. Examples of these latter reactions include the d+^{3}H$\rightarrow$ n+^{4}He fusion used at ITER and at the National Ignition Facility (NIF). Even though there have been many experimental investigations of the cross sections of this reaction, there are still open issues. A first-principles theory based on accurate two-nucleon (NN) and three-nucleon (NNN) forces will provide the predictive power to reduce the uncertainty in the reaction rate at very low temperatures; provide an understanding of the reaction rate dependence on the polarization induced by the strong magnetic fields (characteristic of both inertial and magnetic confinement); and clarify the influence of non-local thermal equilibrium in plasma environments.

In this contribution, we describe the recently introduced *ab initio* many-body approach to reactions on light nuclei [1] that combines the resonating-group method (RGM) [2] with the *ab initio* no-core shell model (NCSM) [3]. We discuss examples of calculations relevant for nuclear astrophysics, ^{7}Be$(p,\gamma)^8$B radiative capture, calculations of the d-^{3}He and d-^{3}H fusion reactions, and investigations of the ground-state (g.s.) resonance of the exotic nucleus ^{7}He.

2 *Ab initio* NCSM/RGM

The *ab initio* nuclear reaction approach that we are developing is an extension of the *ab initio* no-core shell model (NCSM) [3]. The innovation which allows us to go beyond bound states and treat reactions is the use of cluster basis states in the spirit of the resonating-group method,

$$|\Phi^{J^\pi T}_{\nu r}\rangle = \Big[\big(\,|A{-}a\,\alpha_1 I_1^{\pi_1} T_1\rangle\,|a\,\alpha_2 I_2^{\pi_2} T_2\rangle\,\big)^{(sT)}\,Y_\ell\,(\hat{r}_{A-a,a})\Big]^{(J^\pi T)}\,\frac{\delta(r-r_{A-a,a})}{r r_{A-a,a}}\,, \tag{1}$$

in which each nucleon cluster is described within the NCSM. The above translational invariant cluster basis states describe two nuclei (a target and a projectile composed of $A{-}a$ and a nucleons, respectively) whose centers of mass are separated by the relative coordinate $\vec{r}_{A-a,a}$ and that are traveling in a $^{2s}\ell_J$ wave or relative motion (with s the channel spin, ℓ the relative momentum, and J the total angular momentum of the system). Additional quantum numbers characterizing the basis states are parity $\pi = \pi_1\pi_2(-1)^\ell$ and total isospin T. For the intrinsic (antisymmetric) wave functions of the two nuclei we employ the eigenstates $|A{-}a\,\alpha_1 I_1^{\pi_1} T_1\rangle$ and $|a\,\alpha_2 I_2^{\pi_2} T_2\rangle$ of the $(A-a)$- and a-nucleon intrinsic Hamiltonians, respectively, as obtained within the NCSM approach. These are characterized by the spin-parity, isospin and energy labels $I_i^{\pi_i}, T_i$, and α_i, respectively, where $i = 1, 2$. In our notation, all these quantum numbers are grouped into a cumulative index $\nu = \{A{-}a\,\alpha_1 I_1^{\pi_1} T_1;\, a\,\alpha_2 I_2^{\pi_2} T_2;\, s\ell\}$. Finally, we note that the channel states (1) are not antisymmetric with respect to exchanges of nucleons pertaining to different clusters. Therefore, to preserve the Pauli principle one has to introduce the appropriate inter-cluster antisymmetrizer, schematically $\hat{\mathcal{A}}_\nu = \sqrt{\frac{(A-a)!a!}{A!}}\left(1 + \sum_{P\neq id}(-)^p P\right)$, where the sum runs over all possible permutations of nucleons P different from the identical one that can be carried out between two different clusters and p is the number of interchanges characterizing them.

The channel states (1), fully antisimmetrized by the action of the antisymmetrization operator $\hat{A}_\nu$, are used as a continuous basis set to expand the many-body wave function,

$$|\Psi^{J^\pi T}\rangle \;=\; \sum_\nu \int dr r^2\, \hat{\mathcal{A}}_\nu |\Phi^{J^\pi T}_{\nu r}\rangle \frac{[\mathcal{N}^{-1/2}\chi]^{J^\pi T}_\nu(r)}{r}\,, \tag{2}$$

where $\chi^{J^\pi T}_\nu(r)$ represent continuous amplitudes determined by solving the orthogonalized RGM equations:

$$\sum_{\nu'} \int dr' r'^2 [\mathcal{N}^{-\frac{1}{2}}\mathcal{H}\,\mathcal{N}^{-\frac{1}{2}}]^{J^\pi T}_{\nu\nu'}(r,r')\frac{\chi^{J^\pi T}_{\nu'}(r')}{r'} = E\,\frac{\chi^{J^\pi T}_\nu(r)}{r}. \tag{3}$$

Here $\mathcal{N}^{J^\pi T}_{\nu\nu'}(r,r')$ and $\mathcal{H}^{J^\pi T}_{\nu\nu'}(r,r')$, commonly referred to as integration kernels, are respectively the overlap (or norm) and Hamiltonian matrix elements over the antisymmetrized basis (1), *i.e.*:

$$\mathcal{N}^{J^\pi T}_{\nu'\nu}(r',r) = \left\langle \Phi^{J^\pi T}_{\nu' r'}\right|\hat{\mathcal{A}}_{\nu'}\hat{\mathcal{A}}_\nu\left|\Phi^{J^\pi T}_{\nu r}\right\rangle\,,\; \mathcal{H}^{J^\pi T}_{\nu'\nu}(r',r) = \left\langle \Phi^{J^\pi T}_{\nu' r'}\right|\hat{\mathcal{A}}_{\nu'} H \hat{\mathcal{A}}_\nu\left|\Phi^{J^\pi T}_{\nu r}\right\rangle \tag{4}$$

where H is the microscopic $A-$nucleon Hamiltonian and E is the total energy in the center of mass (c.m.) frame. The calculation of the above many-body matrix elements, which contain all the nuclear structure and antisymmetrization properties of the system under consideration, represents the main task in performing RGM calculations. Further details are given in Refs. [4,5]. In the applications presented in Sec. 3 and 4 we employ SRG-evolved [6,7] chiral N^{3}LO [8] NN potentials (SRG-N^{3}LO).

3 Applications

3.1 The ^{7}Be(p,γ)^{8}B radiative capture

The ^{7}Be$(p,\gamma)^8$B radiative capture is the final step in the nucleosynthetic chain leading to ^{8}B and one of the main inputs of the standard model of solar neutrinos. Recently, we have performed the first *ab initio* many-body calculation [9], of this reaction starting from the SRG-N^{3}LO NN interaction with $\Lambda = 1.86$

fm^{-1}. Using p-^{7}Be channel states including the five lowest $N_{\max} = 10$ eigenstates of ^{7}Be (the $\frac{3}{2}^-$ ground and the $\frac{1}{2}^-$,$\frac{7}{2}^-$, and first and second $\frac{5}{2}^-$ excited states), we solved Eq. (3) first with bound-state boundary conditions to find the bound state of ^{8}B, and then with scattering boundary conditions to find the p-^{7}Be scattering wave functions. Former and latter wave functions were later used to calculate the capture cross section, which, at solar energies, is dominated by non-resonant $E1$ transitions from p-^{7}Be S- and D-waves into the weakly-bound ground state of ^{8}B. All stages of the calculation were based on the same harmonic oscillator (HO) frequency of $\hbar\Omega = 18$ MeV, which minimizes the g.s. energy of ^{7}Be. The largest model space achievable for the present calculation within the full NCSM basis is $N_{\max} = 10$. At this basis size, the ^{7}Be g.s. energy is very close to convergence as indicated by a fairly flat frequency dependence in the range $16 \leq \hbar\Omega \leq 20$ MeV, and the vicinity to the $N_{\max} = 12$ result obtained within the importance-truncated NCSM [10, 11]. The choice of $\Lambda = 1.86$ fm^{-1} in the SRG evolution of the N^{3}LO NN interaction leads to a single 2^+ bound state for ^{8}B with a separation energy of 136 keV quite close to the observed one (137 keV). This is very important for the description of the low-energy behavior of the ^{7}Be$(p,\gamma)^8$B astrophysical S-factor, known as S_{17}. We note that the NNN interaction induced by the SRG evolution of the NN potential is repulsive in the Λ-range $\sim$ 1.8-2.1 fm^{-1}, and, in very light nuclei, its contributions are canceled to a good extent by those of the initial attractive chiral NNN force (which is also SRG evolved) [12, 13].

The resulting S_{17} astrophysical factor is compared to several experimental data sets in Figure 1. Energy dependence and absolute magnitude follow closely the trend of the indirect Coulomb breakup measurements of Shümann et al. [14, 15], while somewhat underestimating the direct data of Junghans *et al*. [16]. The resonance, particularly evident in these and Filippone's data, is due to the $M1$ capture, which does not contribute to a theoretical calculation outside of the narrow ^{8}B 1^+ resonance and is negligible at astrophysical energies [17, 18]. The $M1$ operator, for which any dependence upon two-body currents needs to be included explicitly, poses more uncertainties than the Siegert's $E1$ operator. We plan to calculate its contribution in the future. The shape is also quite similar to that obtained within the microscopic three-cluster model [19] (see the dashed line in Fig. 1 (a)) used, after scaling to the data, in the most recent S_{17} evaluation [18]. The contributions from the initial 1^-, 2^- and 3^- partial waves are shown in panel (b) of Fig. 1.

The convergence of our results with respect to the size of the HO model space was assessed by means of calculations up to $N_{\max} = 12$ within the importance-truncation NCSM scheme [10, 11] with (due to computational limitations) only the first three eigenstates of ^{7}Be. The $N_{\max} = 10$ and 12 S-factors are very close. As for the convergence in the number of ^{7}Be states, we explored it by means of calculations including up to 8 ^{7}Be eigenstates in a $N_{\max} = 8$ basis (larger $N_{\max}$ values are currently out of reach with more then five ^{7}Be states). Based on this analysis, we conclude that the use of an

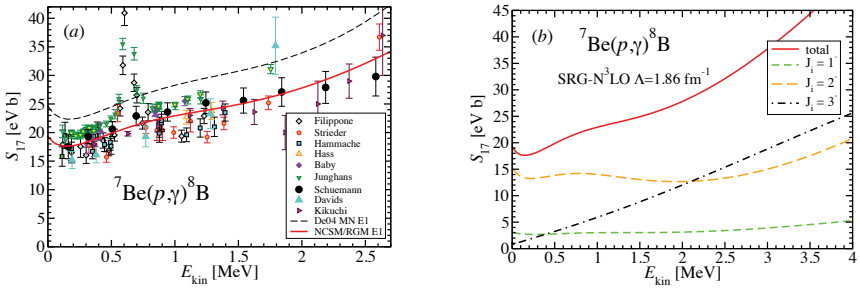

Fig. 1: Calculated ^{7}Be$(p,\gamma)^8$B S-factor as function of the energy in the c.m. compared to data and the microscopic cluster-model calculations of Ref. [19] with the Minnesota (MN) interaction (a). Only $E1$ transitions were considered. Initial-state partial wave contributions are shown in panel (b). Calculation as described in the text.

$N_{\max} = 10$ HO model space is justified and the limitation to five ^{7}Be eigenstates is quite reasonable. Finally, our calculated $S_{17}(0) = 19.4(7)$ MeV b is on the lower side, but consistent with the latest evaluation 20.8 ± 0.7(expt)± 1.4(theory) [18].

3.2 The ^{3}H$(d,n)^4$He and ^{3}He$(d,p)^4$He fusion reactions

The ^{3}H$(d,n)^4$He and ^{3}He$(d,p)^4$He fusion reactions have important implications first and foremost for fusion energy generation, but also for nuclear astrophysics, and atomic physics. Indeed, the deuterium-tritium fusion is the easiest reaction to achieve on earth and is pursued by research facilities directed at reaching fusion power by either inertial (*e.g.*, NIF) or magnetic (*e.g.*, ITER) confinement. Both ^{3}H$(d,n)^4$He and ^{3}He$(d,p)^4$He affect the predictions of Big Bang nucleosynthesis for light-nucleus abundances. In addition, the deuterium-^{3}He fusion is also an object of interest for atomic physics, due to the substantial electron-screening effects presented by this reaction.

In the following we present the first *ab initio* many-body calculations [20] of these reactions starting from the SRG-N^{3}LO NN interaction with $\Lambda = 1.5$ fm^{-1}, for which we reproduce the experimental Q-value of both reactions within 1%. We adopted HO model spaces up to $N_{\max} = 13$ with a frequency of $\hbar\Omega = 14$ MeV. The channel basis includes n-^{4}He (p-^{4}He), d-^{3}H (d-^{3}He), d^*-^{3}H (d^*-^{3}He) and d'^*-^{3}H (d'^*-^{3}He) binary cluster states, where d^* and d'^* denote $^3S_1$-$^3D_1$ and $^3D_2$ deuterium excited pseudostates, respectively, and the ^{3}H (^{3}He) and ^{4}He nuclei are in their ground state.

Figure 2 (left) presents the results obtained for the ^{3}He$(d,p)^4$He S-factor. The deuteron deformation and its virtual breakup, approximated by means of d pseudostates, play a crucial role. The S-factor increases dramatically with the number of pseudostates until convergence is reached for $9d^* + 5d'^*$. The dependence upon the HO basis size is illustrated by the ^{3}H$(d,n)^4$He results of Fig. 2 (right). The convergence is satisfactory and we expect that an $N_{\max}$=15 calculation, which is currently out of reach, would not yield significantly different results. The experimental position of the ^{3}He$(d,p)^4$He S-factor is reproduced within few tens of keV. Correspondingly, we find an overall fair agreement with experiment for this reaction, if we exclude the region at very low energy, where the accelerator data are enhanced by laboratory electron screening. The ^{3}H$(d,n)^4$He S-factor is not described as well with Λ=1.5 fm^{-1}. Due to the very low activation energy of this reaction, the S-factor (particularly peak position and height) is extremely sensitive to higher-order effects in the nuclear interaction, such as three-nucleon force (not yet included in the calculation) and missing isospin-breaking effects in the integration kernels (which are obtained in the isospin formalism). To compensate for these missing higher-order effects in the interaction and reproduce the position of the ^{3}H$(d,n)^4$He S-factor, we performed additional calculations using lower Λ values. This led to the theoretical S-factor of Fig. 2 (right) (obtained for Λ=1.45 fm^{-1}), that is in overall better agreement with data, although it presents a slightly narrower and somewhat overestimated

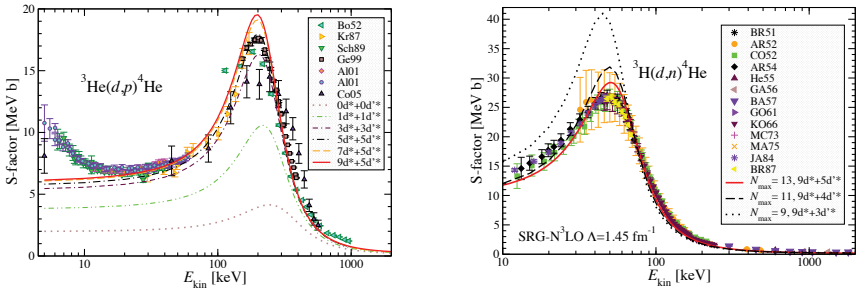

Fig. 2: Calculated S-factor of the ^{3}He$(d,p)^4$He (left) and ^{3}H$(d,n)^4$He (right) reaction compared to experimental data. Left: Convergence with the number of deuterium pseudostates in the $^3S_1$-$^3D_1$ (d^*) and $^3D_2$ (d'^*) channels. Right: Convergence with the size of the basis $N_{\max}$.

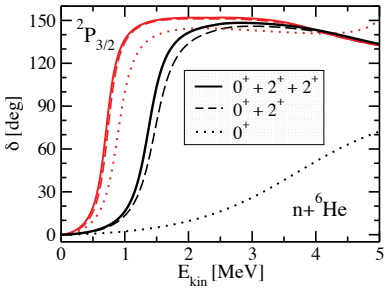

Fig. 3: Dependence of the NCSM/RGM (blue lines) and NCSMC (red lines) ^{6}He + n diagonal phase shifts of the ^{7}He $3/2^-$ g.s. on the number of ^{6}He states included in the binary-cluster basis. The short-dashed, dashed, and solid curves correspond to calculations with the ^{6}He 0^+ g.s. only, $0^+, 2^+$ states, and $0^+, 2^+, 2^+$ states, respectively.

peak. This calculation would suggest that some electron-screening enhancement could also be present in the ^{3}H$(d,n)^4$He measured S factor below 10 keV c.m. energy. However, these results cannot be considered conclusive until more accurate calculations using a complete nuclear interaction (that includes the three-nucleon force) are performed. Work in this direction is under way.

4 No-core shell model with continuum: Application to unbound ^{7}He

We can improve on the NCSM/RGM formalism with a more general unified approach, the no-core shell model with continuum (NCSMC), based on the coupling of the A-nucleon NCSM eigenstates with the NCSM/RGM binary-cluster states. We augment the NCSM/RGM ansatz for the A-body wave function by means of an expansion over A-body NCSM eigenstates $|A\lambda J^\pi T\rangle$ according to:

$$|\Psi_A^{J^\pi T}\rangle = \sum_\lambda c_\lambda |A\lambda J^\pi T\rangle + \sum_\nu \int dr\, r^2 \frac{[\mathcal{N}^{-1/2}\chi]_\nu(r)}{r} \hat{\mathcal{A}}_\nu |\Phi_{\nu r}^{J^\pi T}\rangle, \tag{5}$$

The NCSM sector of the basis provides an effective description of the short- to medium-range A-body structure, while the NCSM/RGM cluster states make the theory able to handle the scattering physics of the system. The discrete, c_λ, and the continuous, $\chi_\nu(r)$ (see Eq. 2) unknowns of the NCSMC wave functions are obtained as solutions of coupled equations that generalize Eq. 3.

This formalism can be applied successfully even to exotic unbound systems like ^{7}He. The ground state of this nucleus is a $3/2^-$ resonance at 0.43 MeV above the neutron and ^{6}He threshold. In Fig. 3, we present the dependence of the $3/2^-$ g.s. phase shifts on the number of ^{6}He eigenstates included in the NCSM/RGM (blue lines) and NCSMC (red lines) calculations. The NCSM/RGM calculation with the ^{6}He target restricted to its g.s. does not produce a ^{7}He $3/2^-$ resonance (the phase shift does not reach 90 degrees). A $^2P_{3/2}$ resonance does appear once the 2_1^+ state of ^{6}He is coupled, and the resonance position further moves to lower energy with the inclusion of the second 2^+ state of ^{6}He. On the contrary, the $^2P_{3/2}$ resonance is already present in the NCSMC calculation that includes four $3/2^-$ NCSM ^{7}He eignestates with only the g.s. of ^{6}He. Adding the 2_1^+ state of ^{6}He generates a modest shift of the resonance to a still lower energy while the second 2^+ state of ^{6}He has no significant influence. We further observe that the resonance position in the NCSMC calculation is lower than the NCSM/RGM one by about 0.7 MeV. This difference is due to the additional correlations brought by the ^{7}He eigenstates that are coupled to the n+^{6}He binary-cluster states in the NCSMC and that compensate for higher excited states of the ^{6}He target omitted in the NCSM/RGM sector of the basis. While NCSM/RGM calculations with a large number of cluster excited states can become prohibitively expensive, the coupling of a few NCSM eigenstates of the composite system is straightforward. More details can be found in Ref. [21].

5 Conclusions and Outlook

We gave an overview of the NCSM/RGM, an *ab initio* many-body approach capable of providing a unified description of structural and reaction properties of light nuclei, by combining the RGM with the use of realistic interactions, and a microscopic and consistent description of the nucleon clusters, achieved via the *ab initio* NCSM. Since the publication of the first results [1,4,22], obtained for nucleon-nucleus collisions, the NSCM/RGM has grown into a powerful approach for the description of light-ion fusion reactions. The formalism has been extended to include two-nucleon (deuteron) projectiles [5], as well as complex reactions with both nucleon-nucleus and deuteron-nucleus channels [20], based on realistic NN interactions. Further extensions of the approach to include the three-nucleon components of the nuclear interaction and three-cluster channel states are under way.

Acknowledgements

Computing support for this work came from the LLNL institutional Computing Grand Challenge program, the Jülich supercomputer Centre and Oak Ridge Leadership Computing Facility at ORNL. Prepared in part by LLNL under Contract DE-AC52-07NA27344. Support from the U. S. DOE/SC/NP (Work Proposal No. SCW1158) and the Natural Sciences and Engineering Research Council of Canada (NSERC) Grant No. 401945-2011 is acknowledged. TRIUMF receives funding via a contribution through the National Research Council Canada. This work is supported in part by the Deutsche Forschungsgemeinschaft through contract SFB 634 and by the Helmholtz International Center for FAIR within the framework of the LOEWE program launched by the State of Hesse.

References

[1] S. Quaglioni and P. Navrátil, *Phys. Rev. Lett.* **101** (2008), 092501
[2] K. Wildermuth and Y. C. Tang, *A unified theory of the nucleus* (Vieweg, Braunschweig) (1977)
[3] P. Navrátil, J. P. Vary, and B. R. Barrett, *Phys. Rev. Lett.* **84** (2000), 5728
[4] S. Quaglioni and P. Navrátil, *Phys. Rev. C* **79** (2009), 044606
[5] P. Navrátil and S. Quaglioni, *Phys. Rev. C* **83** (2011), 044609
[6] S. K. Bogner, R. J. Furnstahl, and R. J. Perry, *Phys. Rev. C* **75** (2007), 061001
[7] R. Roth, S. Reinhardt and H. Hergert, *Phys. Rev. C* **77** (2008), 064003
[8] D. R. Entem and R. Machleidt, *Phys. Rev. C* **68** (2003), 041001
[9] P. Navrátil, R. Roth, and S. Quaglioni, *Physics Letters B* **704** (2011), 379 – 383
[10] R. Roth and P. Navrátil, *Phys. Rev. Lett.* **99** (2007), 092501
[11] R. Roth, *Phys. Rev. C* **79**, (2009) 064324
[12] E. D. Jurgenson, P. Navrátil, and R. J. Furnstahl, *Phys. Rev. Lett.* **103** (2009), 082501
[13] E. D. Jurgenson, P. Navrátil, and R. J. Furnstahl, *Phys. Rev. C* **83** (2011), 034301
[14] F. Schümann *et al.*, *Phys. Rev. Lett.* **73** (2003), 232501
[15] F. Schümann *et al.*, *Phys. Rev. C* **73** (2006), 015806
[16] A. R. Junghans *et al.*, *Phys. Rev. C* **68** (2003), 065803
[17] E. Adelberger E *et al.*, *Rev. Mod. Phys.* **83** (2011), 195
[18] E. Adelberger *et al.*, *Rev. Mod. Phys.* **70** (1998), 1265
[19] P. Descouvemont, Phys. Rev. C **70** (2004), 065802
[20] P. Navrátil and S. Quaglioni, *Phys. Rev. Lett.* **108** (2012), 042503
[21] S. Baroni, P. Navrátil, and S. Quaglioni, arXiv:1210:1897 [nucl-th]
[22] P. Navrátil, R. Roth and S. Quaglioni, *Phys. Rev. C* **82** (2010), 034609